Supporting Information for the article

On the electrochemical properties of the Fe-Ti doped LNMO material $LiNi_{0.5}Mn_{1.37}Fe_{0.1}Ti_{0.03}O_{3.95}$

Pirmin Stüble[a,b], Holger Geßwein[a], Sylvio Indris[a], Marcus Müller[a], and Joachim R. Binder[a]

a: Institute for Applied Materials, Karlsruhe Institute of Technology, 76344 Eggenstein-Leopoldshafen, Germany
b: Helmholtz Institute Ulm, 89081 Ulm, Germany

Table S1: Detailed Information on thermal treatment of all LNMFTO samples and specific surface area of the pristine LNMFTO (A2) and the fast cooled samples FC450 to FC940, according to the BET theory. Specific surface area measurements of the SC samples were omitted, since changes of the particle morphology are very unlikely to occur with slow cooling at temperatures < 650 °C.

Sample	Starting	Thermal Treatment	Specific Surface (BET)
A2	A1	**RT** −300 K/h→ **900 °C (20 h)** −300K/h→ **600 °C (30 h)** −300 K/h→ **RT**	0.82 m²/g
FC460	A2	**RT** −600 K/h→ **460 °C (20 h)** −600K/h→ **RT**	0.75 m²/g
FC500	A2	**RT** −600 K/h→ **500 °C (20 h)** −600K/h→ **RT**	0.74 m²/g
FC540	A2	**RT** −600 K/h→ **540 °C (18 h)** −600K/h→ **RT**	0.75 m²/g
FC580	A2	**RT** −600 K/h→ **580 °C (16 h)** −600K/h→ **RT**	0.78 m²/g
FC620	A2	**RT** −600 K/h→ **620 °C (14 h)** −600K/h→ **RT**	0.77 m²/g
FC660	A2	**RT** −600 K/h→ **660 °C (12 h)** −600K/h→ **RT**	0.79 m²/g
FC700	A2	**RT** −600 K/h→ **700 °C (10 h)** −600K/h→ **RT**	0.76 m²/g
FC740	A2	**RT** −600 K/h→ **740 °C (8 h)** −600K/h→ **RT**	0.77 m²/g
FC780	A2	**RT** −600 K/h→ **780 °C (6 h)** −600K/h→ **RT**	0.78 m²/g
FC820	A2	**RT** −600 K/h→ **820 °C (5 h)** −600K/h→ **RT**	0.80 m²/g
FC860	A2	**RT** −600 K/h→ **860 °C (4 h)** −600K/h→ **RT**	0.83 m²/g
FC900	A2	**RT** −600 K/h→ **900 °C (3 h)** −600K/h→ **RT**	0.83 m²/g
FC940	A2	**RT** −600 K/h→ **940 °C (2 h)** −600K/h→ **RT**	0.84 m²/g
SC460	A2	**RT** −600 K/h→ **460 °C (20 h)** −10 K/h→ **350 °C** −100 K/h→ **RT**	-
SC500	A2	**RT** −600 K/h→ **500 °C (20 h)** −10 K/h→ **350 °C** −100 K/h→ **RT**	-
SC540	A2	**RT** −600 K/h→ **540 °C (18 h)** −10 K/h→ **350 °C** −100 K/h→ **RT**	-
SC580	A2	**RT** −600 K/h→ **580 °C (16 h)** −10 K/h→ **350 °C** −100 K/h→ **RT**	-
SC620	A2	**RT** −600 K/h→ **620 °C (14 h)** −10 K/h→ **350 °C** −100 K/h→ **RT**	-
SC660	A2	**RT** −600 K/h→ **660 °C (12 h)** −10 K/h→ **350 °C** −100 K/h→ **RT**	-
SC700	A2	**RT** −600 K/h→ **700 °C (10 h)** −600 K/h→ **650 °C** −10 K/h→ **350 °C** −100 K/h→ **RT**	-
SC740	A2	**RT** −600 K/h→ **740 °C (8 h)** −600 K/h→ **650 °C** −10 K/h→ **350 °C** −100 K/h→ **RT**	-
SC780	A2	**RT** −600 K/h→ **780 °C (6 h)** −600 K/h→ **650 °C** −10 K/h→ **350 °C** −100 K/h→ **RT**	-
SC820	A2	**RT** −600 K/h→ **820 °C (5 h)** −600 K/h→ **650 °C** −10 K/h→ **350 °C** −100 K/h→ **RT**	-
SC860	A2	**RT** −600 K/h→ **860 °C (4 h)** −600 K/h→ **650 °C** −10 K/h→ **350 °C** −100 K/h→ **RT**	-
SC900	A2	**RT** −600 K/h→ **900 °C (3 h)** −600 K/h→ **650 °C** −10 K/h→ **350 °C** −100 K/h→ **RT**	-
SC940	A2	**RT** −600 K/h→ **940 °C (2 h)** −600 K/h→ **650 °C** −10 K/h→ **350 °C** −100 K/h→ **RT**	-

Table S2: Detailed information on the (auxiliary) components of the cathodes (top) and anodes (bottom).

Component	Type	Manufacturer
Carbon Black	C-NERGY™ SUPER C65	Timcal/Imerys, France
Graphite (cathode)	AGB1010	Superior Graphite Co., USA
Binder (PVDF)	Solef 5130	Solvay, Belgium
Graphite (anode)	SMG-A	Hitachi Chemical, Japan
Binder (Na-CMC)	CRT 2000 PA7	DOW Wolff, Germany
Binder (SBR)	TRD 2001	JSR Micro, Belgium

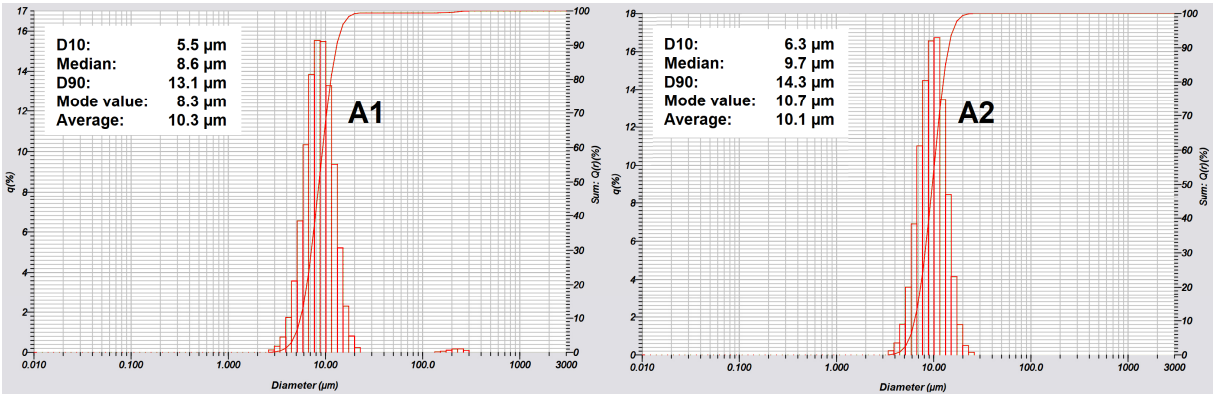

Figure S1: Volumetric particle size distribution for the spherical LNMFTO granules obtained from the second spray drying step (A1) and after the first calcination step (A2). Measurement carried out on a Laser Scattering Particle Size Distribution Analyzer LA-950 (Horiba).

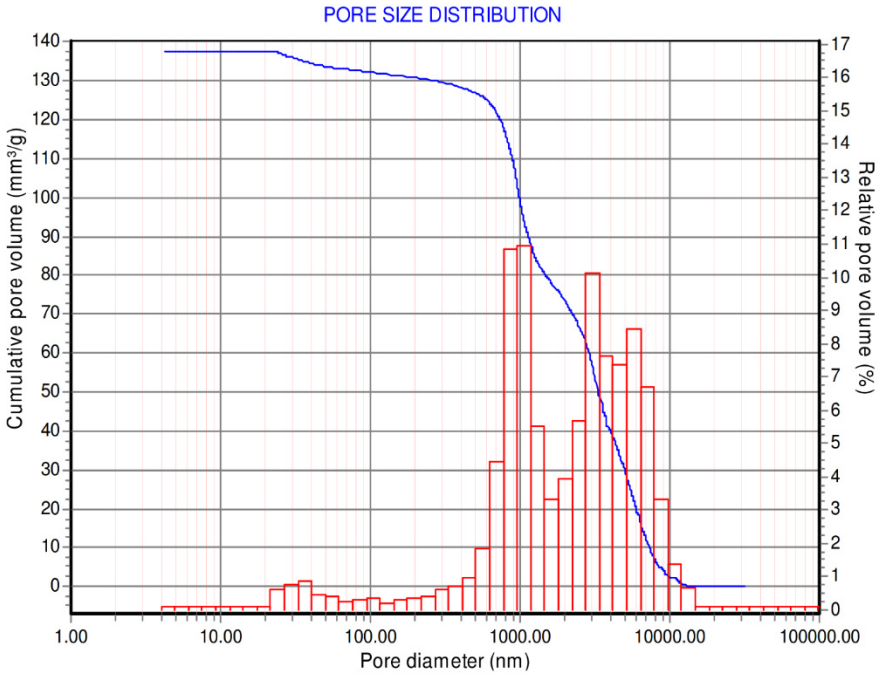

Figure S2: Pore Size distribution of sample A2 obtained from mercury intrusion porosimetry. In accordance with cross section images of the material, pore diameters of ~20 nm to ~1500 nm are attributed to pores inside of the spherical granules. From the corresponding pore volume of ~62 mm³/g, an internal porosity of 20 % is expected. (Calculation for LNMFTO-density of 4.2 g/cm³).

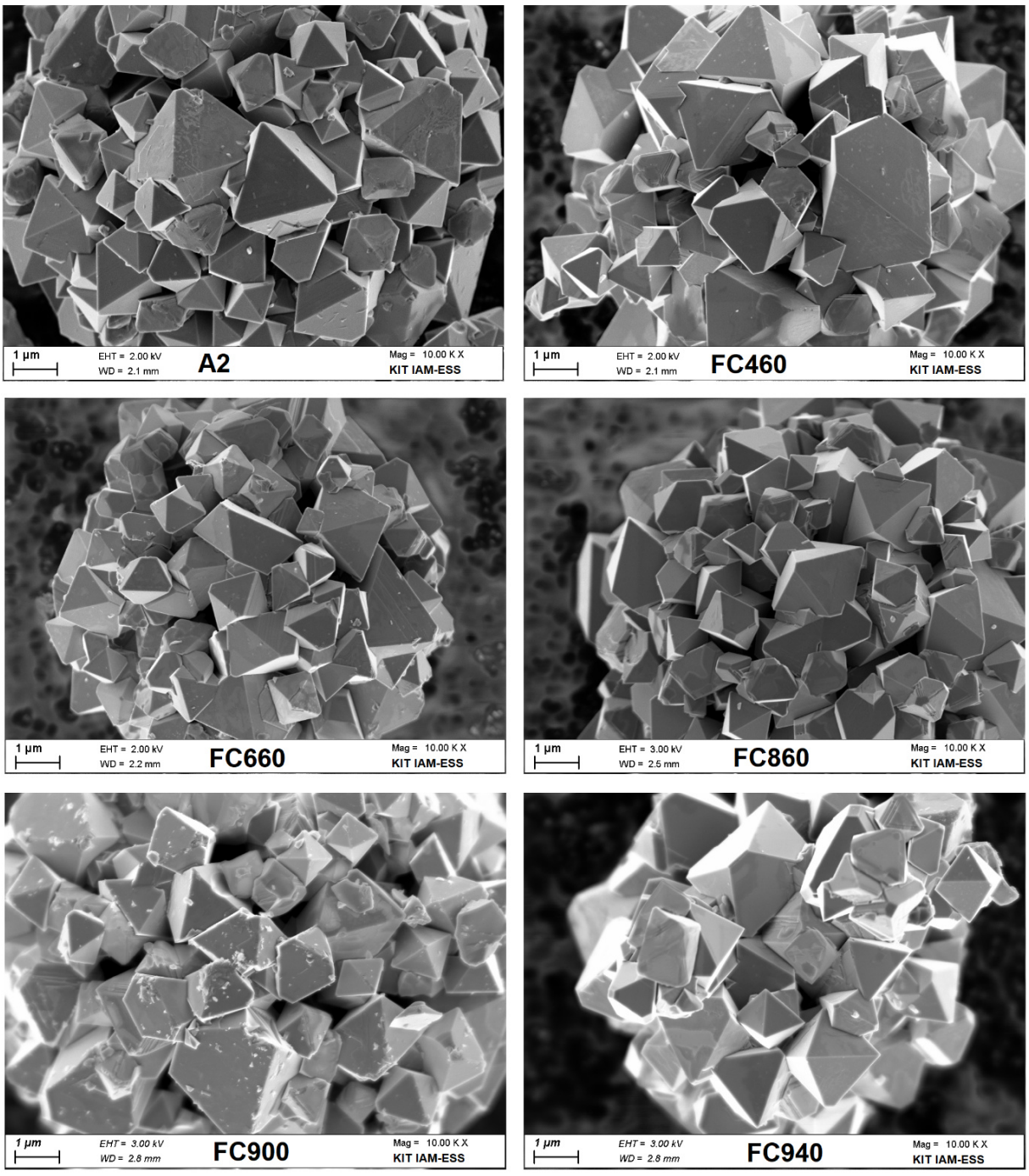

Figure S3: SEM images of the starting material A2 and representative LNMFTO materials calcined at temperatures of 460 °C to 940 °C (FC460 to FC 940). As desired, all granules have a comparable morphology and the vast majority of primary particles shows octahedral shape.

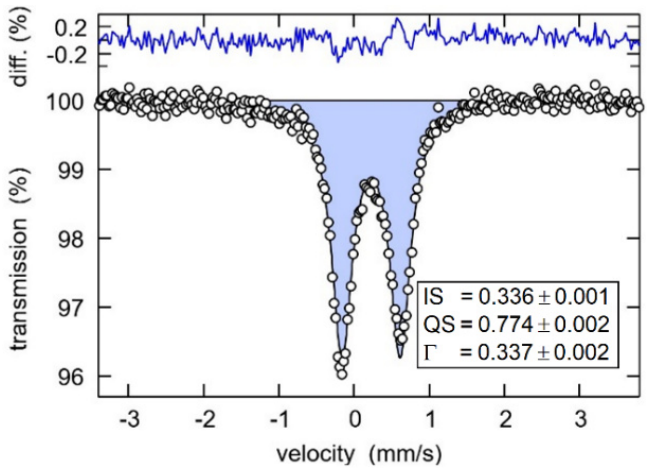

Figure S4: Fe Mößbauer spectrum of sample A2. Experimental data points are shown as white spheres, the overall fit as blue doublet, and the difference as blue line. Fit parameters used to describe the Fe Mößbauer spectrum are shown in the box: isomer shift (IS), quadrupole splitting (QS), and line width (Γ). All values are given in mm/s.

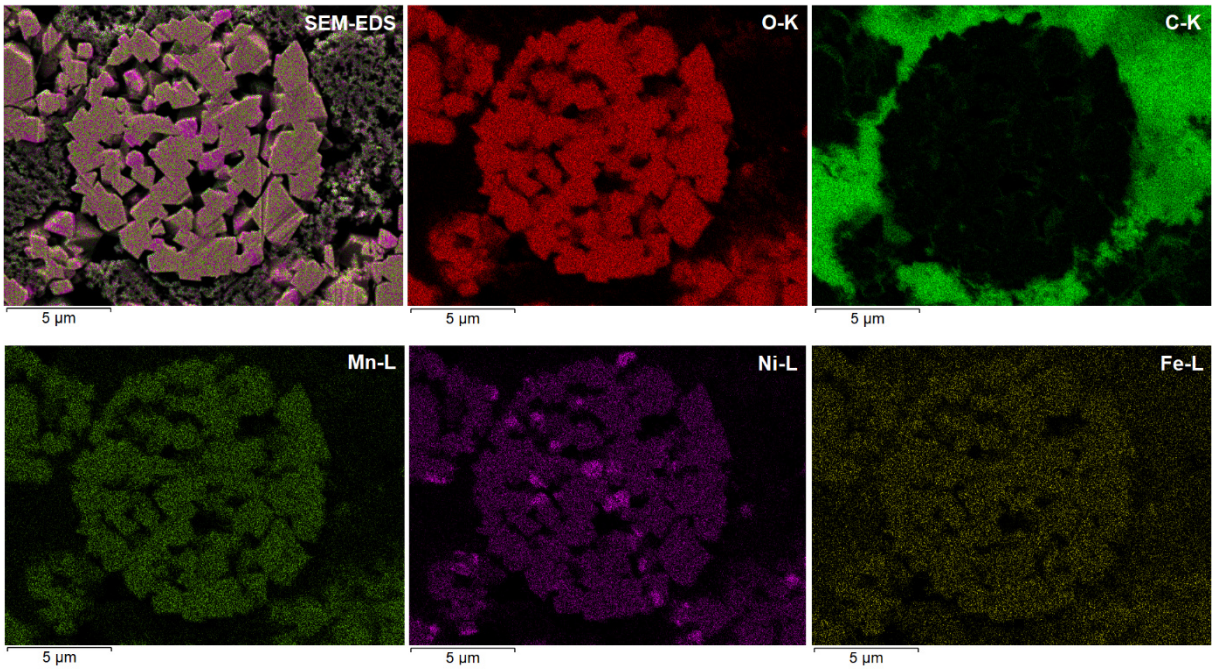

Figure S5: SEM-EDX analysis of the cross-section of a cathode prepared with starting material A2. Areas with increased nickel and reduced manganese content can be assigned to the secondary phase. An accumulation of iron in the secondary phase is not observed. Due to the low titanium concentration, substantial information on its elemental distribution could not be obtained.

Table S3: Results of the Rietveld refinements for the starting material A2 and the fast and slowly cooled LNMFTO series. The uncertainties of the phase fractions are likely to exceed the specified estimated standard deviations due to the overlap of main reflections of both phases.

Sample		LNMFTO ($Fd\bar{3}m$)			$Li_xNi_{1-x}O$ ($R\bar{3}m$)
	R_{wp} [%]	Lattice parameter *a* [pm]	s.o.f. 32*e* (oxygen)	Phase Fraction [wt%]	Phase Fraction [wt%]
A2 (prist.)	2.73	818.61(3)	0.981(6)	93.1(5)	6.9(5)
FC460	3.31	818.32(3)	0.984(6)	94.3(6)	5.7(6)
FC500	3.32	818.25(3)	0.984(6)	94.6(6)	5.4(6)
FC540	3.07	818.23(3)	0.985(6)	94.9(5)	5.1(5)
FC580	2.61	818.35(2)	0.980(6)	95.0(5)	5.0(5)
FC620	2.36	818.45(2)	0.980(6)	95.0(4)	5.0(4)
FC660	2.44	818.65(2)	0.981(6)	94.5(5)	5.5(5)
FC700	3.13	818.97(3)	0.980(6)	92.0(4)	8.0(4)
FC740	2.76	818.17(3)	0.985(6)	90.5(4)	9.5(4)
FC780	3.00	818.34(3)	0.984(6)	89.6(5)	10.4(5)
FC820	2.89	818.42(3)	0.986(6)	89.8(5)	10.2(5)
FC860	2.88	818.50(4)	0.988(6)	90.1(5)	9.9(5)
FC900	2.91	818.55(4)	0.987(6)	89.5(5)	10.5(5)
FC940	2.81	818.64(4)	0.987(6)	90.2(5)	9.8(5)
SC460	2.58	818.36(2)	0.983(6)	94.3(4)	5.7(4)
SC500	2.56	818.29(2)	0.985(6)	94.9(4)	5.1(4)
SC540	2.65	818.24(2)	0.984(6)	95.1(4)	4.9(4)
SC580	2.63	818.23(2)	0.983(6)	94.9(4)	5.1(4)
SC620	2.43	818.24(2)	0.981(6)	95.4(4)	4.6(4)
SC660	2.30	818.22(2)	0.982(6)	95.5(4)	4.5(4)
SC700	2.90	818.38(3)	0.983(6)	95.8(6)	4.2(6)
SC740	3.17	818.29(3)	0.985(6)	94.7(5)	5.3(5)
SC780	3.19	818.31(3)	0.987(6)	94.4(5)	5.6(5)
SC820	3.21	818.34(3)	0.986(6)	93.5(5)	6.5(5)
SC860	3.31	818.35(3)	0.985(6)	93.6(5)	6.4(5)
SC900	3.34	818.40(3)	0.984(6)	93.7(5)	6.3(5)
SC940	3.22	818.45(3)	0.984(6)	95.3(4)	6.7(4)

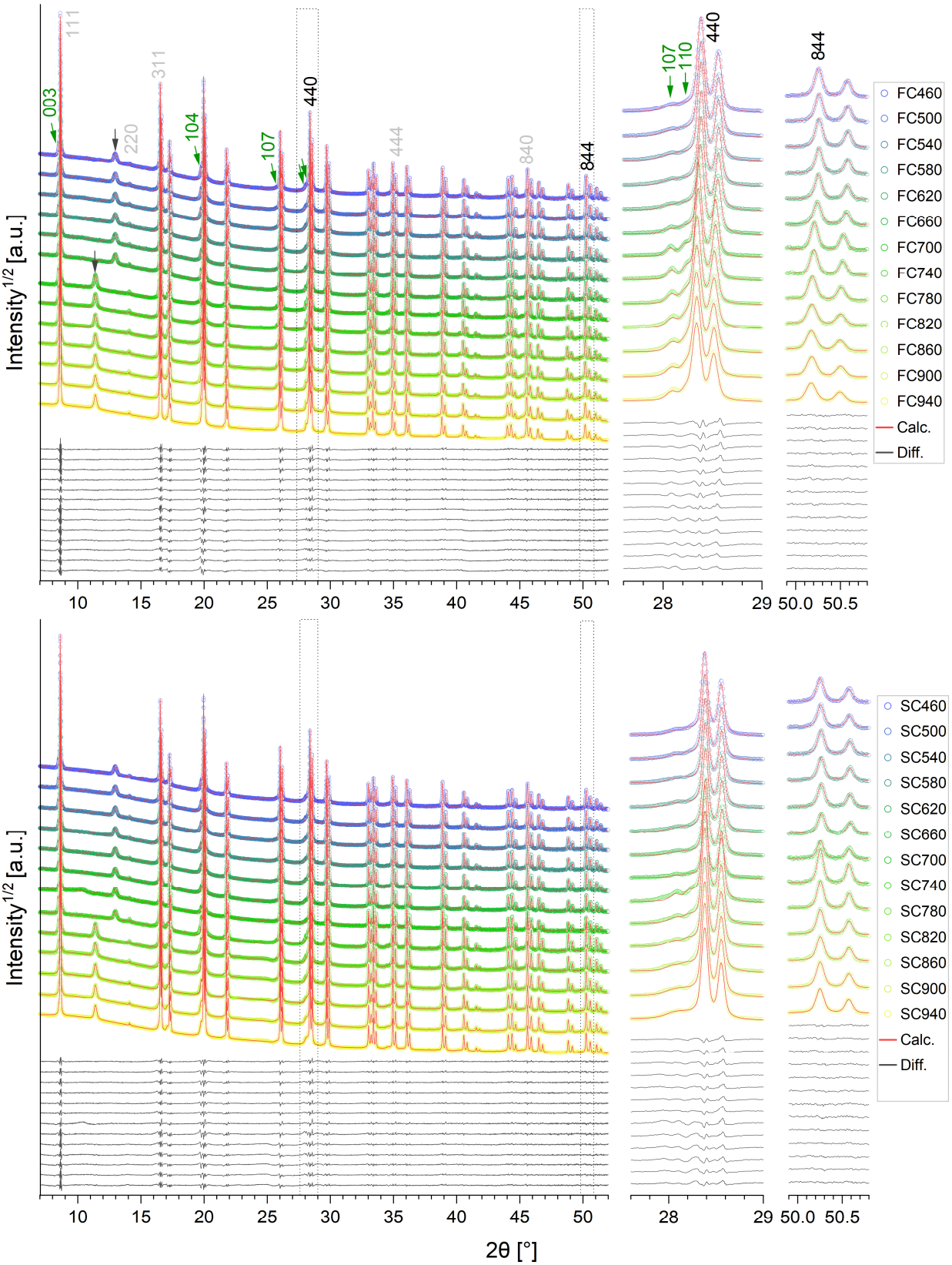

Figure S6: Diffraction patterns and corresponding Rietveld refinement results of the fast (top) and slowly cooled LNMFTO materials (bottom). Selected LNMFTO reflections (space group $Fd\bar{3}m$) are labelled in gray and black. Major reflections of the secondary phase (refined as $Li_xNi_{1-x}O$, space group $R\bar{3}m$) are marked with green arrows and indices. Small changes of the weight fraction of the secondary phase can be seen from the enlarged section around 28.5°. Variations of the lattice parameter of LNMFTO become visible from small shifts of the 844 reflection (section around 50.5°). Double reflections result from $K_{\alpha1}$-$K_{\alpha2}$-splitting. The black arrows indicate contributions of the borosilicate and soda lime glass capillaries used.

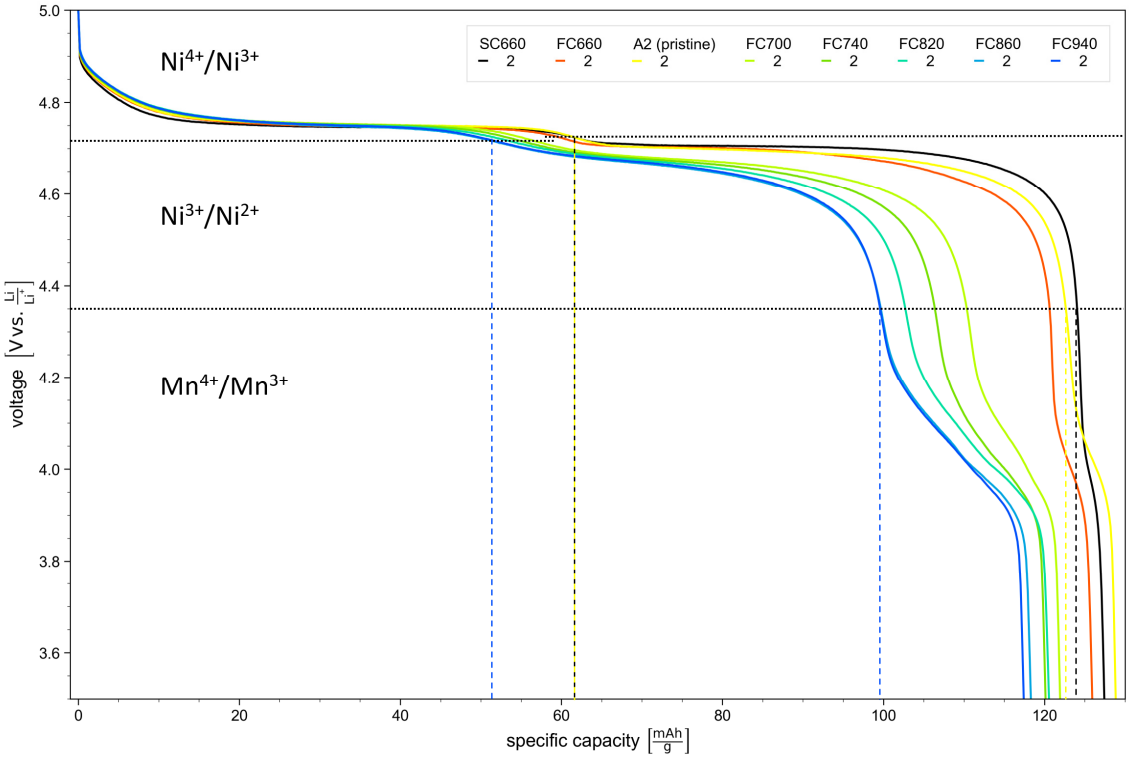

Figure S7: Evaluation of the voltage profiles of the second cycles, shown for samples SC660, A2 and FC660 to FC940. The methodology of previous works of Zhong et al.[28] was applied. Demarcation lines at 4.375 V and 4.72 / 4.73 V (partially ordered / disordered samples) were chosen to partition the capacity in three regions. The results of the evaluation of all samples are listed in the following Table S4.

Table S4: Results of the evaluation of the redox profiles of the second cycle, with individual contributions of Ni and Mn redox couples and the resulting compositions based on $LiNi^{II}_{0.5-x}Mn^{IV}_{1.37-x}Mn^{III}_{2x}Fe_{0.1}Ti_{0.03}O_{3.95}$.

Sample	Ni^{4+}/Ni^{3+}	Ni^{3+}/Ni^{2+}	Cap. Ni total	Mn^{4+}/Mn^{3+}	Cap. total	Ni (rel.)	Mn (rel.)	Composition (calculated)
A2	62	60	122	7	129	94.6%	5.4%	$LiNi_{0.47}Mn_{1.40}Fe_{0.1}Ti_{0.03}O_{3.95}$
FC460	62	61	123	4	127	96.9%	3.1%	$LiNi_{0.48}Mn_{1.39}Fe_{0.1}Ti_{0.03}O_{3.95}$
FC500	62	62	124	4	128	96.9%	3.1%	$LiNi_{0.48}Mn_{1.39}Fe_{0.1}Ti_{0.03}O_{3.95}$
FC540	63	63	126	3	129	97.7%	2.3%	$LiNi_{0.49}Mn_{1.38}Fe_{0.1}Ti_{0.03}O_{3.95}$
FC580	63	63	126	3	129	97.7%	2.3%	$LiNi_{0.49}Mn_{1.38}Fe_{0.1}Ti_{0.03}O_{3.95}$
FC620	62	63	125	3	128	97.7%	2.3%	$LiNi_{0.49}Mn_{1.38}Fe_{0.1}Ti_{0.03}O_{3.95}$
FC660	60	60	120	6	126	95.2%	4.8%	$LiNi_{0.48}Mn_{1.39}Fe_{0.1}Ti_{0.03}O_{3.95}$
FC700	57	53	110	12	122	90.2%	9.8%	$LiNi_{0.45}Mn_{1.42}Fe_{0.1}Ti_{0.03}O_{3.95}$
FC740	56	50	106	14	120	88.3%	11.7%	$LiNi_{0.44}Mn_{1.43}Fe_{0.1}Ti_{0.03}O_{3.95}$
FC780	55	49	104	18	122	85.2%	14.8%	$LiNi_{0.43}Mn_{1.44}Fe_{0.1}Ti_{0.03}O_{3.95}$
FC820	55	47	102	19	121	84.3%	15.7%	$LiNi_{0.42}Mn_{1.45}Fe_{0.1}Ti_{0.03}O_{3.95}$
FC860	53	46	99	19	118	83.9%	16.1%	$LiNi_{0.42}Mn_{1.45}Fe_{0.1}Ti_{0.03}O_{3.95}$
FC900	53	49	102	18	120	85.0%	15.0%	$LiNi_{0.43}Mn_{1.44}Fe_{0.1}Ti_{0.03}O_{3.95}$
FC940	53	47	100	17	117	85.5%	14.5%	$LiNi_{0.43}Mn_{1.44}Fe_{0.1}Ti_{0.03}O_{3.95}$
SC460	62	62	124	6	130	95.4%	3.8%	$LiNi_{0.48}Mn_{1.39}Fe_{0.1}Ti_{0.03}O_{3.95}$
SC500	62	63	125	4	129	96.9%	3.1%	$LiNi_{0.48}Mn_{1.39}Fe_{0.1}Ti_{0.03}O_{3.95}$
SC540	62	64	126	4	130	96.9%	3.1%	$LiNi_{0.48}Mn_{1.39}Fe_{0.1}Ti_{0.03}O_{3.95}$
SC580	63	63	126	4	130	96.9%	3.1%	$LiNi_{0.48}Mn_{1.39}Fe_{0.1}Ti_{0.03}O_{3.95}$
SC620	63	64	127	4	131	96.9%	3.1%	$LiNi_{0.48}Mn_{1.39}Fe_{0.1}Ti_{0.03}O_{3.95}$
SC660	62	62	124	3	127	97.6%	2.4%	$LiNi_{0.49}Mn_{1.38}Fe_{0.1}Ti_{0.03}O_{3.95}$
SC700	61	61	122	5	127	96.1%	3.9%	$LiNi_{0.48}Mn_{1.39}Fe_{0.1}Ti_{0.03}O_{3.95}$
SC740	61	62	123	5	128	96.1%	3.9%	$LiNi_{0.48}Mn_{1.39}Fe_{0.1}Ti_{0.03}O_{3.95}$
SC780	61	61	122	6	128	95.3%	4.7%	$LiNi_{0.48}Mn_{1.39}Fe_{0.1}Ti_{0.03}O_{3.95}$
SC820	60	60	120	7	127	94.5%	5.5%	$LiNi_{0.47}Mn_{1.40}Fe_{0.1}Ti_{0.03}O_{3.95}$
SC860	61	60	121	7	128	94.5%	5.5%	$LiNi_{0.47}Mn_{1.40}Fe_{0.1}Ti_{0.03}O_{3.95}$
SC900	62	58	120	7	127	94.5%	5.5%	$LiNi_{0.47}Mn_{1.40}Fe_{0.1}Ti_{0.03}O_{3.95}$
SC940	62	60	122	6	128	95.3%	4.7%	$LiNi_{0.48}Mn_{1.39}Fe_{0.1}Ti_{0.03}O_{3.95}$